Food and Chemical Toxicology 132 (2019) 110668

Contents lists available at ScienceDirect

Food and Chemical Toxicology

journal homepage: www.elsevier.com/locate/foodchemtox

Bone protective effects of purified extract from *Ruscus aculeatus* on ovariectomy-induced osteoporosis in rats

Lidija Chakuleska[a], Rositza Michailova[a], Aleksandar Shkondrov[b], Vassil Manov[c], Nadya Zlateva-Panayotova[d], Georgi Marinov[d], Reneta Petrova[e], Mariyana Atanasova[f], Ilina Krasteva[b], Nikolay Danchev[a], Irini Doytchinova[f], Rumyana Simeonova[a,*]

[a] Department of Pharmacology, Pharmacotherapy, and Toxicology, Faculty of Pharmacy, Medical University of Sofia, 2, Dunav St, 1000, Sofia, Bulgaria
[b] Department of Pharmacognosy, Faculty of Pharmacy, Medical University of Sofia, 2, Dunav St, 1000, Sofia, Bulgaria
[c] Department of Internal Non-infectious Diseases, Pathology, and Pharmacology, Faculty of Veterinary Medicine, University of Forestry, 10, Kliment Ochridsky Blvd, 1756, Sofia, Bulgaria
[d] Department of Surgery and Radiology, Faculty of Veterinary Medicine, University of Forestry, 10, Kliment Ochridsky Blvd, 1756, Sofia, Bulgaria
[e] National Diagnostic and Research Veterinary Institute, Sofia, Bulgaria, Department: National Center of Animal Health
[f] Department of Chemistry, Faculty of Pharmacy, Medical University of Sofia, 2, Dunav St, 1000, Sofia, Bulgaria

ARTICLE INFO

Keywords:
Osteoporosis
Ruscus aculeatus
Ovariectomized rats
Molecular docking
Oestrogen receptors
Vitamin D receptor

ABSTRACT

Ruscus aculeatus is a source of steroidal saponins that could mimic sex hormones and could help alleviate the risk of fracture in osteoporotic patients. The aim of the present study was to evaluate the *in vitro* effects of an extract from *R. aculeatus* (ERA) on the proliferation of human osteoblast-like SaOS-2 cell line and to investigate the effects of the ERA administered orally for 10 weeks at three doses (50, 100 and 200 mg/kg) on the bone structure of rats with estrogen deficiency induced by bilateral ovariectomy. Bone turnover markers, hormones, histopathological and radiological disturbances were evidenced in the ovariectomized rats. ERA recovered most of the affected parameters in a dose-dependent manner similar to diosgenin and alendronate used as positive comparators. The main active compounds of ERA (ruscogenin and neoruscogenin) were docked into the Vit. D receptor and oestrogen receptors alpha and beta, and stable complexes were found with binding scores equal to those of estradiol and diosgenin.

The findings of this study provide for the first time an insight into the effects of ERA on bone structure and suggest that ERA could be developed as a potential candidate for the prevention of postmenopausal osteoporotic complications.

1. Introduction

Osteoporosis is a progressive, metabolic disease characterized by impaired bone formation resulting in reduced bone mass and microstructure deterioration of bone tissue. Fractures are the most common complication that can occur after insignificant traumas and decrease the quality of life in osteoporotic patients (Ivanova and Vasileva, 2017). The predominant form of the disease is postmenopausal osteoporosis that affects millions of women annually and leads to nearly 3.5 million fractures in Europe (Hernlund et al., 2013). Therefore, the timely prevention and appropriate treatment of this condition are of paramount importance in reducing bone resorption and fracture risk in postmenopausal women. The long-term use of current osteoporosis treatments, however, can cause serious side effects, including increased cardiovascular risk and risk to develop different types of cancer (Chakuleska et al., 2018). The antiresorptive oral bisphosphonates (such as alendronate (ALN), used as a positive control in this study) have long been established as first-line therapy for women with postmenopausal osteoporosis but have further been reported to strongly impair liver function and cause organ damage (Halabe et al., 2000). These limitations of the conventional osteoporosis drugs have recently been shifting the scientific focus to exploring alternative remedies from natural sources as a nontherapeutic approach for improving bone health and reducing the risk of fractures. A systematic review and meta-

* Corresponding author.
E-mail addresses: lcakuleska@gmail.com (L. Chakuleska), rositsa.a.mihaylova@gmail.com (R. Michailova), a_shkondrov@abv.bg (A. Shkondrov), vmanov@ltu.bg (V. Manov), n_zlateva@mail.bg (N. Zlateva-Panayotova), g.marinov@ltu.bg (G. Marinov), reneta_petrova@abv.bg (R. Petrova), mariyanda@gmail.com (M. Atanasova), krasteva.ilina@abv.bg (I. Krasteva), nikolai.danchev@gmail.com (N. Danchev), doytchinova@gmail.com (I. Doytchinova), rvitanska@gmail.com (R. Simeonova).

https://doi.org/10.1016/j.fct.2019.110668
Received 13 May 2019; Received in revised form 4 July 2019; Accepted 8 July 2019
Available online 09 July 2019
0278-6915/

Abbreviations

ACP	acid phosphatase
ALN	alendronate
ALP	alkaline phosphatase
BMC	bone marrow channel
β-CTx	Beta-CrossLaps
BMD	bone mineral density
Ca	calcium
CAT	catalase
DSG	diosgenin
DTNB	2,2- Dinitro-5,5 dithiodibenzoic acid
ECLIA	electro-chemi-luminescence immunoassay
ER	estrogenic receptor
ERA	extract from Ruscus aculeatus
EST	estradiol
FBS	foetal bovine serum
GSH	reduced glutathione
ISO	International Organization for Standardization
LD	lethal dose
LPO	lipid peroxidation
MDA	malonedialdehyde
OC	osteocalcin
OP	osteoporosis
OVX	ovariectomy
P	phosphorus
PTH	parathyroid hormone
RSG	ruscogenin
NRS	neoruscogenin
SI	soy isoflavones
TBARS	thiobarbituric acid reactive substances
TCA	trichloroacetic acid
VDR	Vitamin D receptor

analysis provided further evidence for the positive correlation between fruit and vegetable intake, so-called “Healthy dietary pattern”, on one hand, and bone health and bone mineral density (BMD), on the other (Denova-Gutiérrez et al., 2018).

A great number of studies elucidate the mechanisms underlying the beneficial effects of phytoestrogens, including soy isoflavones (SI), in managing osteoporosis or other menopausal symptoms (Zheng et al., 2016). These bioactive phytoderivatives show different binding affinity to the oestrogen receptors (ER) and mimic most actions of the endogenous estradiol through trans-activation or trans-repression of its downstream target genes (Turner et al., 2007). Phytoestrogens may inhibit the differentiation of osteoclasts and stimulate osteoblastic bone formation (Oršolić et al., 2018). Plants that contain steroidal saponins could, therefore, be good candidates for antiosteoporotic nutraceuticals or phytopharmaceuticals due to the strong resemblance in the chemical structures of the related sapogenins and the oestrogen hormones (Cos et al., 2003). Low levels of oestrogens cause decreased bone formation by different mechanisms including suppressed osteoblast activity, increased bone resorption through increased osteoclast activity, augmented oxidative stress in bones and intestines (Kander et al., 2017) and thus impaired calcium absorption (Diaz de Barboza et al., 2015).

The plant-derived steroidal sapogenin diosgenin (DSG) has been shown to inhibit osteoclastogenesis, to stimulate the osteogenic activity of osteoblasts *in vitro*, and to exert antiosteoporotic effects in rats *in vivo* (Folwarczna et al., 2016).

Ruscus genus is a rich source of bioactive steroidal saponins. The genus includes many species spread throughout Europe. *R. aculeatus* or “butcher's broom” is the most widely distributed and the most studied species as phlebotherapeutic agent (Masullo et al., 2016). The rhizome extract is used for the treatment of chronic venous insufficiency, varicose veins, haemorrhoids, orthostatic hypotension, colitis, diarrhoea, and is used locally against inflammation and arthritis (Masullo et al., 2016). In the 17th century, the English herbalist Nicholas Culpepper used butcher's broom to help the healing of fractured bones (Tobyn, 2013). The underground parts of *Ruscus* plants are a source of steroidal saponins. The diol aglycones (25*R*)-spirost-5-en-1*β*,3*β*-diol, named ruscogenin (RSG), and spirost-5,25(27)-dien-1*β*,3*β*-diol, named neoruscogenin (NRG) (Fig. 1), were first isolated from the subterranean parts of *R. aculeatus* and described in 1955–1957 (Masullo et al., 2016). RSG and NRS closely resemble DSG's and estradiol's (EST) structure (Fig. 1). This structure similarity might mimic oestrogen-like effects on the bones and prevent them from fractures.

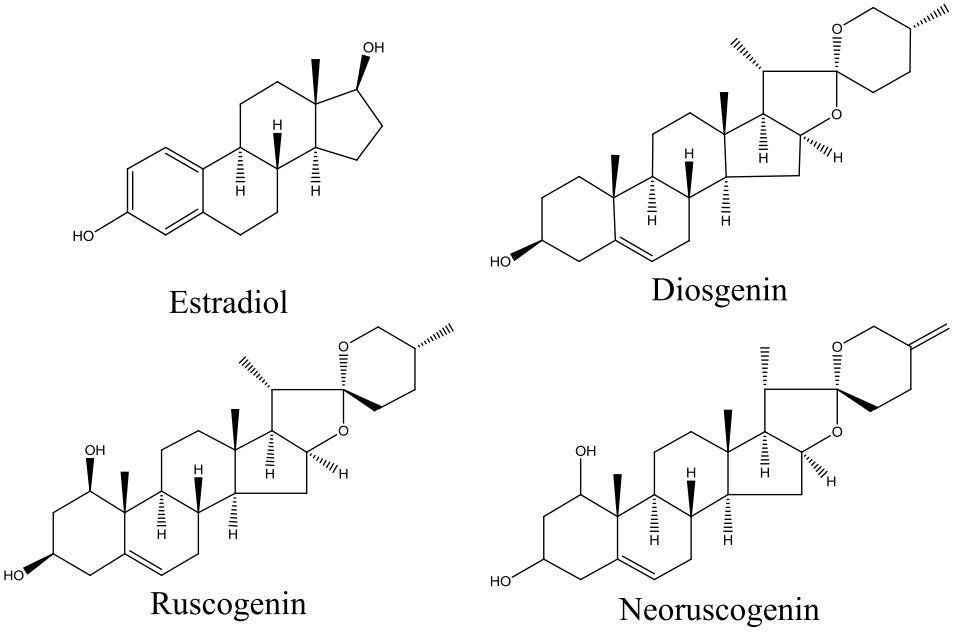

Fig. 1. Chemical structures of estradiol (EST), and the spirostanol aglycones diosgenin (DSG), ruscogenin (RSG) and neoruscogenin (NRS).

To the best of our knowledge, the bone-protective effects of *Ruscus aculeatus* have not been studied yet. On this ground, we set out to investigate the biological effects of a highly purified *R. aculeatus* rhizome extract (ERA) in an ovariectomy (OVX) induced osteoporosis rat model in a comparative manner to DSG and ALN, used as positive controls.

2. Materials and methods

2.1. Plant material

Rhizomes and roots of *Ruscus aculeatus* L. (Liliaceae) were purchased from a herbal pharmacy in Sofia, Bulgaria (certificate № 42117/13.04.2018). The plant material (1 kg) was grinded, sieved (3 mm) and treated with methylene chloride (3 L) to remove the lipophilic constituents. The defatted drug was further percolated with 80% EtOH (10 L) and then with water (5 L) (Peneva et al., 2000). The extracts were combined and evaporated to eliminate the solvent. The residue was lyophilized and the obtained dry extract (drug extract ratio, DER 4.17:1) was named ERA (240 g). The steroid saponins' content was analysed by an HPLC method, described in European Pharmacopoeia 9.0 (Europe Council, 2017). It was found that ERA contained 20% saponins expressed as ruscogenin and neoruscogenin.

2.2. Chemicals

Alendronate sodium salt, dioscin, diosgenin, trichloroacetic acid (TCA), and 2-thiobarbituric acid (TBA) were purchased from Sigma Chemical Co. (Taufkirchen, Germany). 2,2- Dinitro-5,5′-dithiodibenzoic acid (DTNB) was obtained from Merck (Darmstadt, Germany). All reagents used were of analytical grade.

2.3. Animals

Three months old female Wistar rats (initial body weight 200–250 g) were purchased from the National Breeding Centre, Sofia, Bulgaria. The rats were housed under standard laboratory conditions with free access to water and standard pelleted rat food 53–3, produced according to ISO 9001:2008. Seven days' acclimatization was allowed before the commencement of the study and their health was monitored regularly by a veterinary physician. The study design was approved by the Bulgarian Agency of Food Safety (permission № 208) and the principles stated in the European Convention for the Protection of Vertebrate Animals used for Experimental and other Scientific Purposes (ETS 123) (Council of Europe, 2007) were strictly followed throughout the experiment.

2.4. In vitro study on SAOS-2 cell line viability

Cell lines and culture conditions. The effects of ERA, DSG, and ALN on cell proliferation were tested *in vitro* on the human SAOS-2 osteosarcoma cells with osteoblast-like properties. Cells were cultivated in a modified McCoy's medium supplemented with 15% foetal bovine serum (FBS) and incubated under standard conditions of 37 °C and 5% humidified CO_2 atmosphere.

MTT dye reduction assay. The metabolic activity of SAOS-2 was determined using a standard MTT-based colorimetric assay for evaluating cell viability. Exponential-phase cells were harvested and seeded (100 µl/well) in 96-well plates at a density of 1.5×10^5/ml. Following 24 h incubation, cells were treated with serial dilutions of the studied substances in various concentration ranges, as follows:

- ERA: 400.00–25.00 µg/ml (Rauly-Lestienne et al., 2017)
- ALN: 150.00–9.38 µM (Cheng et al., 2004)
- DSG: 2.50–0.50 µM (Men-Luh et al., 2005)

Following exposure time of 72 h, a filter-sterilized MTT substrate solution (5 mg/mL in FBS) was added to each well of the culture plate. A further 1–4 h incubation allowed the formation of purple insoluble precipitates of the formazan dye. The latter were dissolved in an isopropyl alcohol solution containing 5% formic acid prior to absorbance measurement at 550 nm. Values were blanked against MTT-and isopropanol solution and normalized to the mean value of untreated control (assumed as 100% cell viability).

2.5. Acute oral toxicity of ERA

Acute oral toxicity of ERA was performed according to the simplified Lorke method (Lorke, 1983) in order to choose appropriate doses for the *in vivo* study.

2.6. Pharmacological assessment

2.6.1. Design of the in vivo experiment

Forty-two female three months old Wistar rats were randomly divided into seven groups of six animals each. Six rats were abdominally resected without removal of the ovaries and served as a control (sham-operated group). The remaining 36 animals were subjected to bilateral ovariectomy (OVX) (Bazzigaluppi et al., 2018). Prior to surgical manipulation, the animals were anaesthetized by intramuscular (i.m.) application of the mixture ketamine/xylazine (75 mg/kg b.w. and 10 mg/kg b.w., respectively (Oršolic et al., 2018).

One week after the surgical procedure, the animals were divided into groups as follows:

Group 1: Sham-control, treated with saline (0.9% NaCl);
Group 2: Ovariectomized (OVX) control rats, treated with saline (0.9% NaCl);
Group 3: OVX rats receiving ERA (50 mg/kg b.w.);
Group 4: OVX rats receiving ERA (100 mg/kg b.w.);
Group 5: OVX rats receiving ERA (200 mg/kg b.w.);
Group 6: OVX rats receiving dioscin (DSG), as a first positive control, (60 mg/kg b.w.) (Tao et al., 2016).
Group 7: OVX rats treated with ALN, the second positive control (3 mg/kg b.w./week) (Mustafa et al., 2018).

All treatments were administered daily by oral gavage for 10 weeks. Only ALN was given orally once a week. During the experimental period, the weight of each animal was checked weekly. On the 35th day after overnight starvation, the animals from all groups were anaesthetized with i.m. application of ketamine/xylazine mixture, blood was taken from a saphenous vein, and biochemical markers of calcium homeostasis and bone turnover were measured. The radiological examination was performed on 35th and 70th day.

On the 71st day after overnight starvation, the animals from all groups were sacrificed by decapitation. Blood, intestines, livers, and bones were taken, organs rinsed with ice-cold saline buffer and stored on ice for further investigation.

2.6.2. Markers of calcium homeostasis

On the 35th and 71st-day blood was collected in tubes containing clot activator. After centrifugation at $3000 \times g$ for 10 min serum was separated and stored at −20 °C for further evaluation.

Calcium (Ca) and phosphorus (P) were measured using commercially available kits for biochemical analyser Mindray – BP 120 (China). 25-OH Vit. D, parathyroid hormone (PTH), and estradiol-E2 levels were analysed using electrochemiluminescence immunoassay "ECLIA" with kits for immunoassay analyser (Cobas-Roche, Basel, Switzerland).

2.6.3. Markers of bone turnover

Markers of bone formation - osteocalcin (OC) and alkaline phosphatase (ALP), and markers of bone resorption - Beta-CrossLaps (β-CTx) and acid phosphatase (ACP) were analysed on the 35th and 71st day

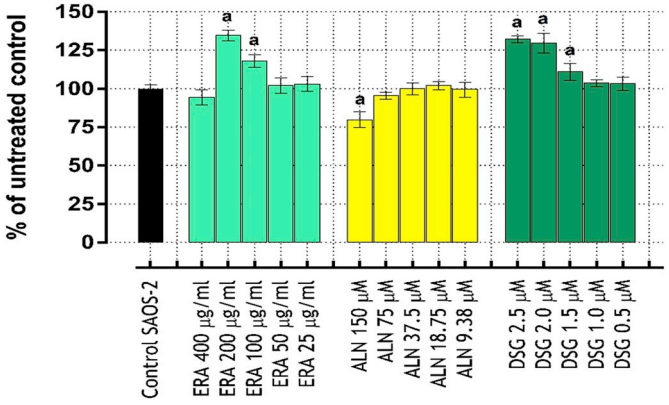

Fig. 2. Viability of SAOS-2 cells following 72 h exposure to various concentrations of the tested compounds; [a] $p < 0.05$ vs control.

with commercially available kits. ALP and ACP were measured using biochemical analyser Mindray–BP 120 (China). OC and β-CTx were analysed using "ECLIA" with kits for immunoassay analyser (Cobas-Roche, Basel, Switzerland).

For the following experiments the excised right femurs, livers, and intestines were washed with cold (4 °C) saline solution, blotted dry, weighed and homogenized with appropriate buffers. Femurs were firstly frozen at −80 °C, then crushed in a porcelain mortar and ground in a laboratory mill (disintegrator type).

2.6.4. Markers of oxidative stress

Lipid peroxidation was determined by measuring the rate of production of thiobarbituric acid reactive substances (expressed as MDA equivalents) using the method described by Polizio and Pena (Polizio and Peña, 2005).

GSH was assessed by measuring of non-protein sulfhydryls after precipitation of proteins with trichloroacetic acid (TCA), using the method of Bump et al. (1983).

2.7. Radiological evaluation

Anaesthetized animals from all groups were examined radiologically on the 35th and 70th day using Eckenmeyer INNOVET X-ray machine. The scanning protocol used an X-ray energy of 53 kVp and 6 mAs. The X-ray images were digitalized by ADS Solo Agfa System.

2.8. Histological examination of rat's bone

Femurs and tibia of the rats from all groups were removed and fixed in 10% buffered formalin for 48 h. Fixed bones were placed in decalcification solution (formic acid) for 14 days and then processed according to the classic paraffin method. They were stained with haematoxylin and eosin (H&E) (Bancroft and Gamble, 2008). Histological changes were observed and photo-documented on Euromex BioBlue microscope.

2.9. Molecular docking to oestrogen receptors (ERs) and vitamin D receptor (VDR)

The molecules of DSG, RSG and NRS were downloaded from PubChem and docked into the X-ray structures of human oestrogen receptor alpha and beta forms (*ERα* and *ERβ*, pdb id: 5WGD, R = 1.8 Å and 3OLS, R = 2.2 Å) (Möcklinghoff et al., 2010; Speltz et al., 2018) and human vitamin D receptor (VDR) (pdb id: DB1, R = 1.8 Å) (Rochel et al., 2000). The docking was performed by GOLD v. 5.2.2 (CCDC Ltd., Cambridge, UK) at the following settings: scoring function GoldScore, flexible ligand, flexible binding site, radius of the binding site 6 Å, toggled water molecule (HOH788 for ERα, HOH228 for ERβ, HOH501, HOH505, and HOH506 for VDR), 100 GA runs. The contact residues of the binding site were set as flexible. For ERα these are Met343, Glu353, Leu387, Leu391, Arg394, Phe404, His524, Leu525, and Met528; for ERβ – Met295, Glu305, Leu339, Leu343, Arg346, Phe356, His475, Leu476 and Met479; for VDR – Tyr143, Leu233, Ser237, Ile271, Arg274, Ser278, Trp286, Leu313, His305, His397. Estradiol (EST) was used as a reference molecule in both ERs and the active form of vitamin D - 1α,25-dihydroxy vitamin D_3 ($1,25(OH)_2D_3$; VD3) was used in VDR.

2.10. Statistical analysis

For the *in vitro* cell culture study a semi-logarithmic "dose-response" curves were computed using nonlinear regression in GraphPad Prism® 6.0.

Statistical software "MEDCALC" was used for the analysis of the data. For the *in vivo* experiments, the data are expressed as mean ± SEM of six rats in each group. The significance of the data was assessed using the nonparametric Mann-Whitney *U* test. Values of $p \leq 0.05$ were considered statistically significant.

3. Results

3.1. In vitro study on SAOS-2 cell line viability

The viability of SAOS-2 cells after 72 h exposure to various concentrations of ERA and the two controls DSG and ALN is given in Fig. 2. As is evident, the reference drug ALN had no beneficial impact on cell proliferation in the tested concentration range (150.00–9.38 µM), whereas DSG and the ERA change moderately the metabolic activity in a dose-specific manner. The most pronounced stimulatory effects were observed in the 200 µg/ml ERA-treated group (second highest concentration) and in the 2.5 µM and 2.0 µM DSG-treated groups. At lower exposure concentrations, both ERA and DSG produced a weak dose-dependent induction of osteoblastic activity that gradually subsides to that of the control group. However, *ca.* 10% inhibition of cell growth was observed at the maximum treatment dose of ERA (400 µg/ml). An equivalent antiproliferative effect had ALN at the highest tested concentration (150 µM). When comparing changes in cell metabolic activity at different concentrations of DSG and the ERA, a correlation was observed.

3.2. Acute oral toxicity test of ERA

The LD_{50} p.o. for ERA was calculated to be 2121 mg/kg in female rats. According to Hodge and Sterner toxicity scale, the obtained value of $LD_{50} > 2000$ mg/kg classified the ERA as slightly toxic herbal medicine (Derelanko and Hollinger, 2002). Doses of 50, 100, and 200 mg/kg which represent approximately 1/40, 1/20 and 1/10 of LD_{50}, respectively, were used in the subsequent pharmacological assessment.

3.3. Body weight changes

The changes in body weight during the experiment are shown in Table 1. Throughout the experiment, all animals gained weight. Compared with the first-week Sham-control rats and ALN treated rats gained weight by 36% ($p < 0.05$), OVX rats and animals treated with 50 mg/kg ERA gained by 46% ($p < 0.05$). Higher doses of ERA, 100 and 200 mg/kg, as well as DSG, led to a significant body weight gain (BWG) by 38% and 28% respectively. Compared to the control group during the tenth week, the highest BWG was observed in OVX rats and rats treated with the lowest dose of ERA, by 30% and 33% respectively ($p < 0.05$), while the final BWG in the treated with the highest dose ERA was lower by 24% ($p < 0.05$). When compared to the OVX group at the 10th week, the groups treated with 100 mg/kg and 200 mg/kg ERA showed lower BWG by 18% and 41% respectively. BWG in DSG

Table 1
Changes in body weight gain (BWG).

Animal group ($n = 6$)	Mean body weight (g)		
	Initial (1st week)	Final (10th week)	Change
Sham	236.6 ± 4.2	322.1 ± 12.2	85.5[a]
OVX	244.6 ± 7.8	356.1 ± 10.3	111.5[ab]
ERA 50	248.6 ± 6.6	362.6 ± 11.6	114.0[ab]
ERA 100	240.3 ± 4.5	331.3 ± 9.1	91.0[ac]
ERA 200	231.2 ± 7.7	296.4 ± 11	65.4[abc]
DSG	235.4 ± 12	300.4 ± 6.2	65.0[abc]
ALN	236.0 ± 8.9	320.3 ± 8.6	82.3[ac]

Treatment groups are as described in Section 2.6.1.

treated animals was similar to the changes in the BW at the highest dose of ERA (200 mg/kg).

Data are expressed as mean ± SEM of six rats ($n = 6$). For comparison between groups, the Mann-Whitney U test was performed. [a] $p < 0.05$ vs first week; [b] $p < 0.05$ vs sham-control group at tenth week; [c] $p < 0.05$ vs OVX group at tenth week.

3.4. Parameters of calcium homeostasis

The changes in parameters of calcium homeostasis are shown in Table 2. At the 35th day, the levels of calcium (Ca) were higher ($p < 0.05$) in untreated and all treated OVX rats than in the Sham-control group. In the OVX group, the Ca level was higher by 18%, compared to the control. The Ca level in the lowest dose of ERA (50 mg/kg) was similar to the Ca level in the OVX group. In the groups treated with the higher doses of ERA and DSG, Ca was higher ($p < 0.05$) by 13% and 11% respectively, than in the OVX group. When comparing with the sham-control group calcium concentration in ALN-treated group was higher by 23% ($p < 0.05$) and similar to the OVX group.

The phosphorus (P) level was higher ($p < 0.05$) by 25% and by 23% in OVX rats and in the rats treated with 50 mg/kg ERA respectively, compared to the control group. Treatment of OVX rats with ERA 100 mg/kg and 200 mg/kg decreased significantly the P level by 28% and 25% respectively, compared to the OVX group. Similarly, DSG and ALN decreased the serum P level by 16% and 18%, respectively compared to the OVX group.

The level of 25-OH Vit. D (Vit. D total) was lower ($p < 0.05$) in OVX rats, in 50 mg/kg, and in 100 mg/kg ERA-treated groups by 52%, and 50%, respectively, compared to the control group. Rats treated with 200 mg/kg ERA, DSG and ALN had higher ($p < 0.05$) levels of Vit. D by 50%, 45%, and 79%, respectively, compared to the OVX group.

Apart from the control group, the levels of the parathyroid hormone (PTH) were lower in all experimental groups, even lower than the detection limit of the method.

Estradiol levels were also very low (under the limit of detection) in all groups, incl. in the controls.

At the end of the experiment, on the 71st day, all investigated parameters in all experimental groups were similar to the control group.

3.5. Markers of bone turnover

OVX resulted in a significant change in bone turnover markers discerned by an increase ($p < 0.05$) in OC level by 81%, in ALP activity by 202%, in ACP activity by 97%, and in β-CTx concentration by 27%, compared to the control group (Table 3). OVX rats treated with 50 mg/kg ERA showed similar to OVX rats' changes in the biochemistry. Administration of ERA at 100 mg/kg led to a significant decrease ($p < 0.05$) of the activity of ALP and ACP by 14% and 38% respectively, compared to the OVX group. Administered at 200 mg/kg ERA decreased significantly ($p < 0.05$) the OC level by 24%, ALP by 25%,

Table 2
Biomarkers of calcium homeostasis measured on the 35th day and on the 71st day in the control, OVX and different treated groups.

	35th day						
	Control	OVX	ERA 50	ERA 100	ERA 200	DSG	ALN
Ca, mmol/L	2.02 ± 0.13	2.38 ± 0.06[a]	2.28 ± 0.05[a]	2.69 ± 0.19[ab]	2.67 ± 0.17[ab]	2.64 ± 0.12[ab]	2.48 ± 0.17[a]
P, mmol/L	1.84 ± 0.11	2.29 ± 0.18[a]	2.26 ± 0.17[a]	1.64 ± 0.24[b]	1.72 ± 0.25[b]	1.92 ± 0.13[b]	1.88 ± 0.22
25-OH Vit. D, nmol/L	49.29 ± 4.91	23.73 ± 4.2[a]	23.87 ± 4.16[a]	24.84 ± 6.06[a]	35.58 ± 8.15[ab]	34.43 ± 2.72[ab]	42.43 ± 8.78[b]
PTH, pmol/L	1.34 ± 0.052	< 1.2	< 1.2	< 1.2	< 1.2	< 1.2	< 1.2
Estradiol E2, pmol/L	< 18.4	< 18.4	< 18.4	< 18.4	< 18.4	< 18.4	< 18.4
	71st day						
	Control	OVX	ERA 50	ERA 100	ERA 200	DSG	ALN
Ca, mmol/L	2.08 ± 0.17	2.18 ± 0.12	2.20 ± 0.14	2.22 ± 0.12	2.27 ± 0.19	2.24 ± 0.14	2.12 ± 0.16
P, mmol/L	1.84 ± 0.11	1.91 ± 0.08	1.89 ± 0.12	1.74 ± 0.34	1.72 ± 0.15	1.82 ± 0.13	1.82 ± 0.06
25-OH Vit. D, nmol/L	51.12 ± 3.24	48.23 ± 3.86	50.22 ± 2.24	52.36 ± 8.06	51.31 ± 6.62	49.36 ± 3.46	50.12 ± 2.78
PTH, pmol/L	1.36 ± 0.052	1.31 ± 0.036	1.30 ± 0.032	1.28 ± 0.026	1.29 ± 0.028	1.32 ± 0.031	1.42 ± 0.022
Estradiol E2, pmol/L	< 18.4	< 18	< 18.4	< 18.4	< 18.4	< 18.4	< 18.4

Treatment groups are as described in Section 2.5.1. Data are expressed as mean ± SEM of six rats ($n = 6$). For comparison between groups, the Mann-Whitney U test was performed. [a] $p < 0.05$ vs Sham-control group on the 35th day; [b] $p < 0.05$ vs OVX-control group on the 35th day.

Table 3
Biomarkers of bone turnover measured on the 35th day and on the 71st day in control, OVX and different treated groups.

	Control	35th day					
		OVX	ERA 50	ERA 100	ERA 200	DSG	ALN
OC, ng/mL	12.09 ± 1.63	20.48 ± 2.54[a]	21.23 ± 3.4[a]	17.74 ± 3.74[a]	15.63 ± 1.17[ab]	14.97 ± 1.26[b]	16.17 ± 2.22[b]
ALP, U/L	102.3 ± 18.6	308.6 ± 12.3[a]	302.2 ± 16.6[a]	268.3 ± 14.6[ab]	231.2 ± 18.3[ab]	186.6 ± 10.8[ab]	164.1 ± 8.6[ab]
ACP, U/L	23.6 ± 2.32	46.4 ± 4.64[a]	42.6 ± 5.02[a]	28.7 ± 6.24[b]	22.2 ± 3.88[b]	19.5 ± 3.66[b]	18.1 ± 6.6[b]
β-CTx, pg/mL	7.80 ± 0.68	9.88 ± 0.44[a]	6.64 ± 0.38[a]	9.15 ± 0.41[a]	8.89 ± 0.32[ab]	7.87 ± 0.42[b]	7.62 ± 0.26[b]
	71st day						
	Control	OVX	ERA 50	ERA 100	ERA 200	DSG	ALN
OC, ng/mL	13.42 ± 2.26	15.23 ± 1.13	14.52 ± 1.2	14.56 ± 1.36	14.44 ± 1.23	13.86 ± 2.23	13.62 ± 3.22
ALP, U/L	89.65 ± 8.27	99.36 ± 4.56	92.5 ± 6.8	87.22 ± 3.31	82.56 ± 4.44	81.45 ± 6.23	84.24 ± 6.12
ACP, U/L	24.38 ± 3.61	32.12 ± 8.66	28.8 ± 9.0	30.21 ± 8.06	28.26 ± 6.42	26.28 ± 5.42	22.22 ± 4.48
β-CTx, pg/mL	8.12 ± 0.52	8.68 ± 0.66	8.32 ± 0.4	7.89 ± 0.36	7.88 ± 0.43	8.02 ± 0.52	7.92 ± 0.61

Treatment groups are as described in Section 2.5.1. Data are expressed as mean ± SEM of six rats ($n = 6$). For comparison between groups, the Mann-Whitney U test was performed. [a] $p < 0.05$ vs Sham-control group at the 35th day; [b] $p < 0.05$ vs OVX-control group at the 35th day.

ACP by 52% and β-CTx by 11% compared to the OVX rats. The DSG-treated group showed a significant decline ($p < 0.05$) in the OC concentration by 27%, in the ALP and ACP activities by 40% and 58% respectively, and decrease of β-CTx value by 20%, compared to the OVX rats. ALN also decreased ($p < 0.05$) the OC level by 21%, ALP by 47%, ACP by 61%, and β-CTx by 23%, compared to the OVX group.

At the end of the experimental period, there were no statistically significant differences in the measured parameters between the groups.

3.6. Markers of oxidative stress

The OVX-induced oxidative stress in the liver, intestines, and bones was proved by the increased ($p < 0.05$) formation of MDA by 18%, 10%, and 13%, respectively, compared to the sham control group (Fig. 3A). OVX decreased ($p < 0.05$) the GSH level in liver, intestines, and bones by 19%, 17%, and 21%, respectively, in comparison with the Sham-control group (Fig. 3B). The lowest dose of ERA (50 mg/kg) did not show protective effects regarding oxidative stress markers on the investigated organs in OVX rats. ALN also raised ($p < 0.05$) the MDA content by 19% in all tested organs and decreased ($p < 0.05$) the hepatic and bone GSH level by 18% compared to the control rats. Ten weeks' treatment of OVX rats with 100 mg/kg ERA led to a significant decline ($p < 0.05$) in MDA formation only in the liver of exposed animals by 22%, but increased ($p < 0.05$) the GSH content in all investigated organs. In liver, intestines, and bones, the GSH levels were higher by 10%, 15%, and 13%, respectively than the GSH level in the OVX group. The highest dose of ERA had better effects on the markers of oxidative stress. MDA level declined ($p < 0.05$) in the liver, intestines, and bones of the treated animals by 25%, 18%, and 16%, respectively, while the GSH content improved ($p < 0.05$) by 15%, 25%, and 22%, respectively, compared to the OVX rats. DSG administered at dose 30 mg/kg to the OVX rats reduced ($p < 0.05$) the MDA quantity by 21%, 19% and 14% in the liver, intestines, and bones, respectively, compared to OVX animals. In the same time, DSG significantly ($p < 0.05$) augmented the GSH level in those organs by 17%, 21%, and 30%, respectively, compared to the OVX rats.

3.7. Radiological examination

The first radiological examination was made 35 days after the ovariectomy. The X-ray images showed the differences in the bone structures in OVX rats compared to the normal control group. As shown in Fig. 4B, C and 4D the animals in OVX group and group treated with the lowest dose of ERA, had decreased bone density, especially in the region of proximal femur and deformities in the proximal tibias. The cortical line was not clear (Fig. 4D). In the proximal tibia (Fig. 4B) and in the femoral neck (Fig. 4C) small areas with increased radiolucency were observed. Radiological changes in the higher doses ERA (100 and 200 mg/kg), DSG and ALN treated groups were not observed (Fig. 4E, F, G, and H).

One month later a new radiological examination was done Figs. 6 and 7. In the OVX group deformation of the pelvic bones and bone lysis (destruction) were observed (Fig. 6B). An absence of a clear demarcation between the compact and the bone marrow channel and reduced bone density of the last lumbar vertebrae were also observed (Fig. 6B). Decreased femoral bone density, deformation of the tibia curvature,

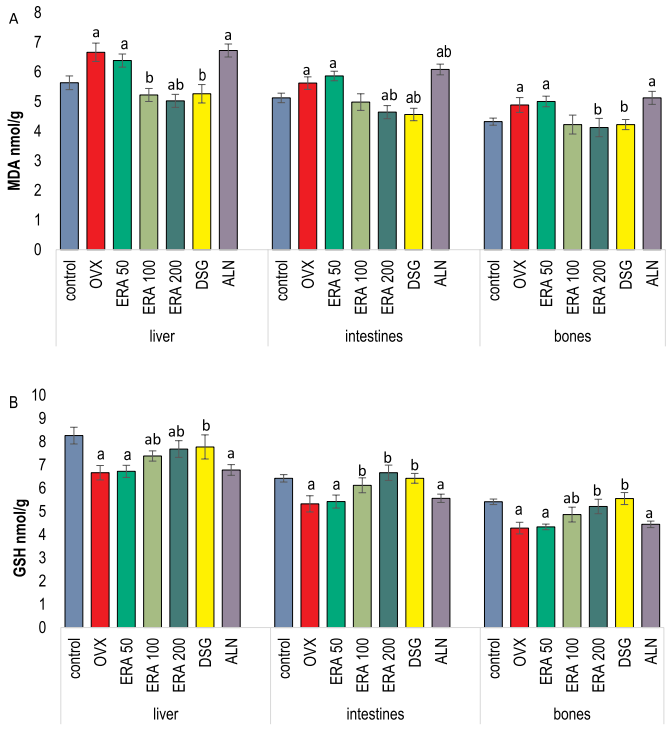

Fig. 3. MDA quantity (A) and GSH level (B) in the sham-control group, OVX group, and in all treated OVX groups. Treatment groups are as described in Section 2.6.1. Data are expressed as mean ± SEM of six rats ($n = 6$). For comparison between groups, the Mann-Whitney U test was performed. [a] $p < 0.05$ vs Sham-control group; [b] $p < 0.05$ vs OVX-control group.

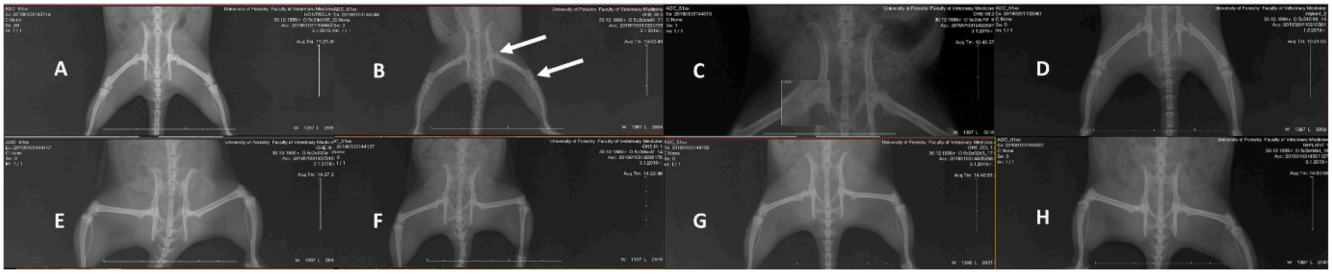

Fig. 4. Radiological evaluation on the 35th day. **A.** Image of the hind limbs and tail of the control rat; **B.** Radiograph of the hind limbs and tail of the OVX rat with decreased bone density in the region of proximal femur, deformities in the proximal tibia; **C.** Femoral neck of OVX rat, small areas with increased radiolucency; **D.** Radiograph of an animal treated with 50 mg/kg ERA with increased diameter of bone marrow channel (BMC); **E, F, G,** and **H** - images of animals treated with the higher doses ERA, DSG, and ALN without radiological changes in the hind limbs and tail.

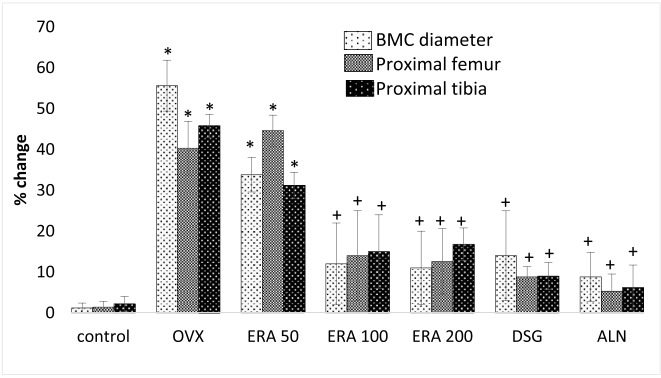

Fig. 5. Radiological changes in the diameter of the BMC, proximal femur, and proximal tibia in % on the 35th day. Treatment groups are as described in Section 2.6.1. Data are expressed as mean ± SEM of six rats (n = 6). For comparison between groups, the Mann-Whitney *U* test was performed. $^{*}p < 0.05$ vs Sham-control group; $^{+}p < 0.05$ vs OVX-control group.

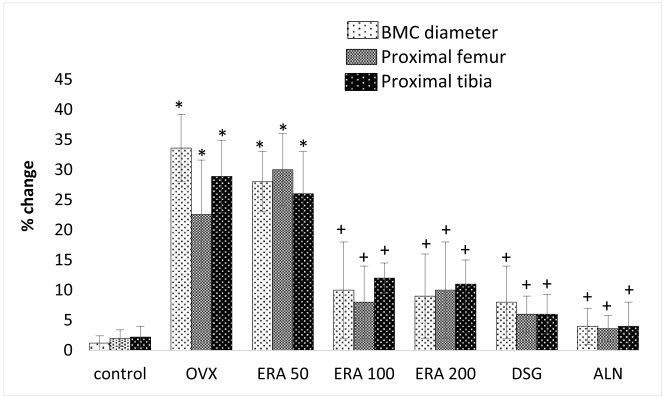

Fig. 7. Radiological changes in the BMC diameter, proximal femur, and proximal tibia in % on the 70th day. Treatment groups are as described in Section 2.6.1. Data are expressed as mean ± SEM of six rats (n = 6). For comparison between groups, the Mann-Whitney *U* test was performed. $^{*}p < 0.05$ vs Sham-control group; $^{+}p < 0.05$ vs OVX-control group.

lack of clear cortical line, and increased diameter of the bone marrow canal of the femur were also visible (Fig. 6C). In the same group many osteophytes in the area of the stifle joint were discovered (Fig. 6C). Radiograph of an animal treated with 50 mg/kg ERA (Fig. 6D), showed a lack of clear cortical line and increased diameter of the BMC. Radiographs of the animals from the groups protected with the higher doses ERA, DSG, and ALN did not show deformations and expansion of the BMC. The compact line was very clearly outlined (Fig. 5E, F, G, and H).

3.8. Histopathological changes

Bones from the sham-control animals (Fig. 8A and B) showed unchanged bone structure, corresponding to the bone type of the anatomical area of the incision. Femoral diaphysis was built of lamellar bone tissue, forming a well-developed tubular compact substance and scarce central, sponge-like, cancellous tissue. The compact substance had solid, concentrically located, mineralized lamellas, forming osteons with a centrally located Havers canals. Individual osteons were connected by slanting Folkman's channels. The epiphyseal plate of the femurs and tibias, as well as the femoral head, were consisted of thin compact substance and well-developed spongious substance, with bone grafts and interlocking barriers. Osteocytes were located in lacunas, distributed between irregular bones lamellas formed as a network. Periosteal and endosteal surfaces were intact. Bone marrow spaces ware visible between the trabeculae (Fig. 8A and B).

In the OVX group and the lowest dose ERA group (Fig. 8C, D, and E) the femoral diaphysis showed a thinner compact substance, with smaller osteons and enlarged Havers canals. The irregular colouration of the bone tissue due to the presence of areas with advanced decalcification was observed. These changes, along with the observed

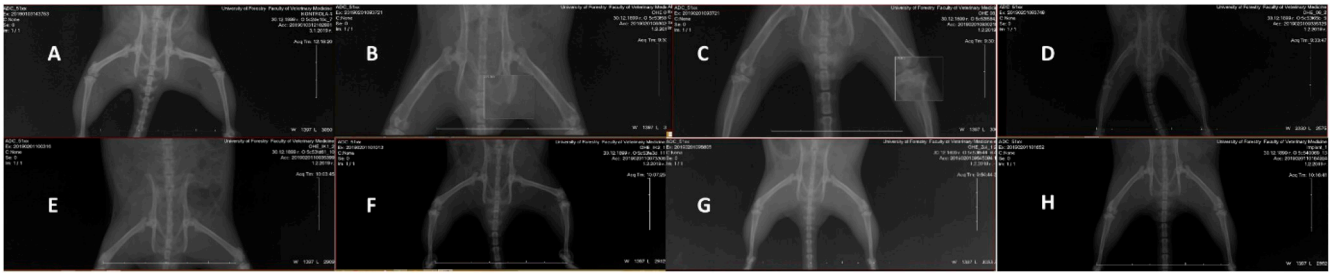

Fig. 6. Radiological evaluation on the 70th day. **A.** Image of the hind limbs and tail of the control rat; **B.** Deformation of pelvic bones and bone lysis (destruction); **C.** Decreased bone density of the femur and tibiae and osteophytes; **D.** Lack of clear cortical line in the lowest dose ERA treated group**; E, F, G** and **H.** Images of animals treated with the higher doses ERA, DSG, and ALN without radiological changes in the hind limbs and tail.

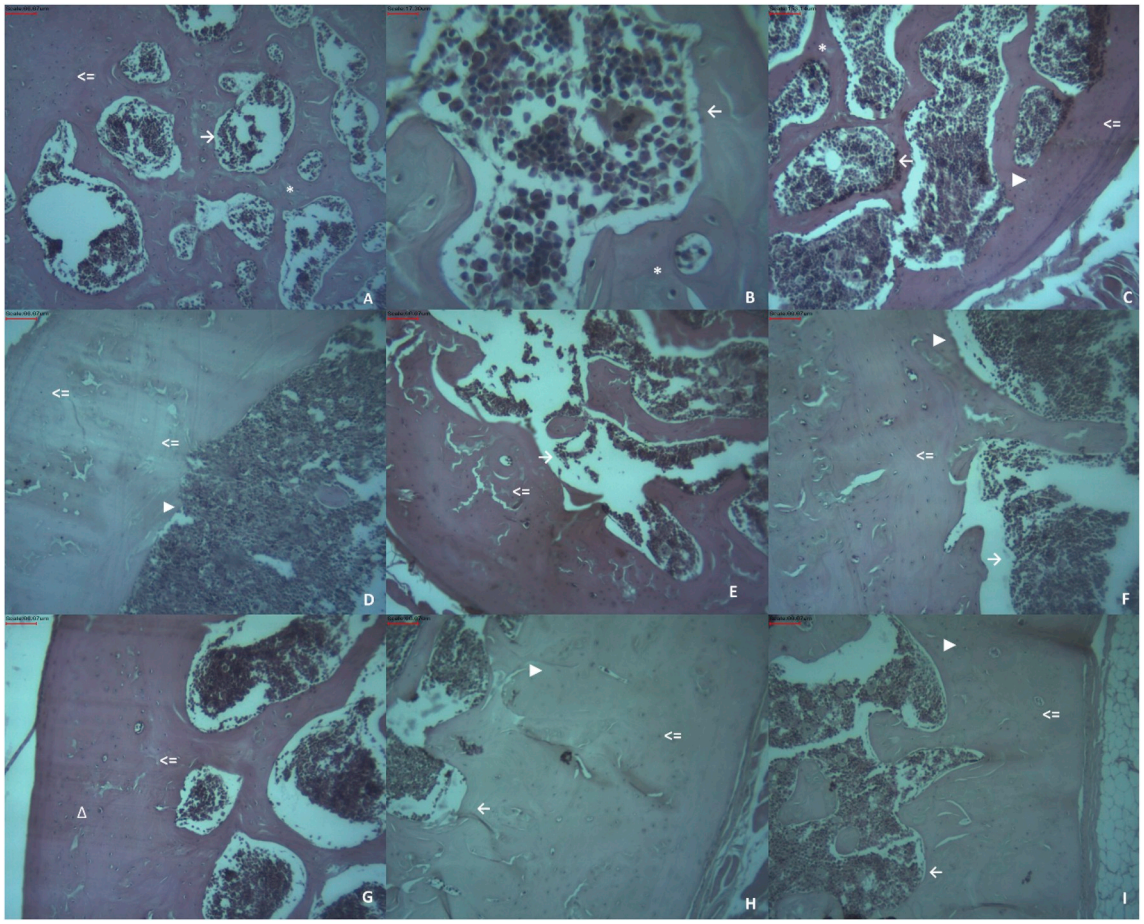

Fig. 8. Histopathological examination of the stained with H&E bone's sections. Bone tissue of a femoral head of the sham-control group (**A** and **B**). Osteoporotic tissue of a femoral head (**C**) and diaphysis (**D**) of the OVX rats. Bone tissue of a femoral diaphysis of OVX rats, treated with ERA 50 mg/kg (**E**); ERA 100 mg/kg (**F**); ERA 200 mg/kg (**G**); DSG (**H**) and ALN (**I**). Compact substance (= >) and bone marrow (→); endosteal (►) and periosteal (Δ) surfaces; trabeculae of a cancellous bone (*).

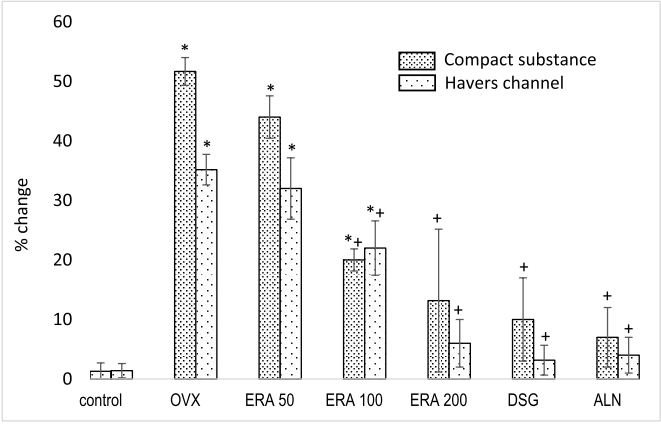

Fig. 9. Histopathological changes in compact substance and Havers channels in % in the experimental groups. Treatment groups are as described in Section 2.6.1. Data are expressed as mean ± SEM of six rats (n = 6). For comparison between groups, the Mann-Whitney *U* test was performed. $^{*}p < 0.05$ vs Sham-control group; $^{+}p < 0.05$ vs OVX-control group.

osteoclastic osteolysis, forming cavities with various shapes and sizes, gave a porous appearance of the tissue. This porousness was complemented by the osteolytic changes visible in the endosteal and periosteal surfaces. In the metaphyseal zones of the femur and tibia, as well as in the femoral head, the architecture of the osteons in the spongious substance was found to be impaired. Apart from chaotic and thinned, not well-communicated trabeculae, enlarged bone marrow spaces were also visible (Fig. 8C, D and E).

The bone fragments of the OVX rats, treated with ERA 100 and 200 mg/kg showed signs of regeneration of the disturbed histological structures (Fig. 8F and G). The thickness of the compact area of the femoral bone diaphysis was increased, the colouration of the bone lamellas was more homogenous compared to the OVX animals and the number and size of the intracortical cavities were significantly reduced. In the metaphyseal areas, as well as in the femoral head, a thickening of the osteons in the cancellous bone was established as compared to the untreated OVX rats. On the endosteal surface of the spongious tissue, singular irregularities were found. The recovery effect of ERA on the porous bones was better expressed in OVX animals receiving the higher dose (200 mg/kg) (Fig. 8G).

In the osteoporotic rats treated with DSG (Fig. 8H) recovery of the size of the compact substance and the thickness of the lamellas in the cancellous bone (based on an increased number of osteoblasts and osteocytes), as well as the shaping of the normal trabecular architecture were found.

The OVX animals treated with ALN showed a high degree of recovery of the porous structures. The established histological picture showed features of the normal bone. The formed osteons were of a thickness approximating that of the control group (Fig. 8I). Single small cavities located in the cortical area of the bone were also seen. The endosteal surface was relatively smooth with the presence of several uneven spots.

Table 4
The highest GoldScores of the studied compounds docked in ERα, ERβ, and VDR.

	ERα	ERβ	VDR
EST/VD3	82.24[a]	81.02[b]	101.38[c]
DSG	56.14	53.41	58.15
RSG	57.55	54.69	62.27
NRS	59.33	56.73	54.98

[a] RMSD = 0.3676 Å.
[b] RMSD = 0.2850 Å.

3.9. Molecular docking study

The highest docking scores of EST/VD3, DSG, RSG and NRS in ERα, ERβ and VDR are given in Table 4. The binding poses corresponding to the highest-scored complexes are presented in Fig. 10. EST makes several hydrogen bonds with ERs. The two OH-groups act as anchors at both ends of the molecule. The 3-OH is involved in a dense network of hydrogen bonds with Glu353, Leu387, Arg394 from ERα and one molecule of structural water. The corresponding residues in ERβ are Glu305, Leu339, Arg346. The 17-OH makes one hydrogen bond with His524 from ERα and His475 from ERβ.

DSG, RSG, and NRS have close binding scores but lower than the score of EST. The highest-scored binding poses of these compounds are similar to those of EST (Fig. 10B and D) but only one anchor exists here: the 3β-OH makes only one hydrogen bond with His524 from ERα and His475 from ERβ. The lower number of hydrogen bonds between these compounds and ERs explains the lower binding score than this of EST.

The 1-OH of VD3 forms one hydrogen bond with Arg274, which itself is hydrogen bonded to a water molecule. The 3-OH of $1,25(OH)_2D_3$ makes two hydrogen bonds with Trp143 and Ser278. The 25-OH group is hydrogen bonded to His305 and His397. The C6–C7 single bond is in *trans* conformation with 30° deviation from the planar geometry (Rochel et al., 2000). The docked poses of the studied compounds follow this binding orientation, although there is enough space in the binding site to take planar geometry. The 1β-OH and 3β-OH of RSG and NRG make one hydrogen bond each with Ser278 and Tyr143, respectively. 3β-OH of RSG forms an additional hydrogen bond with one of the structural water molecules stabilizing the complex. DSG is

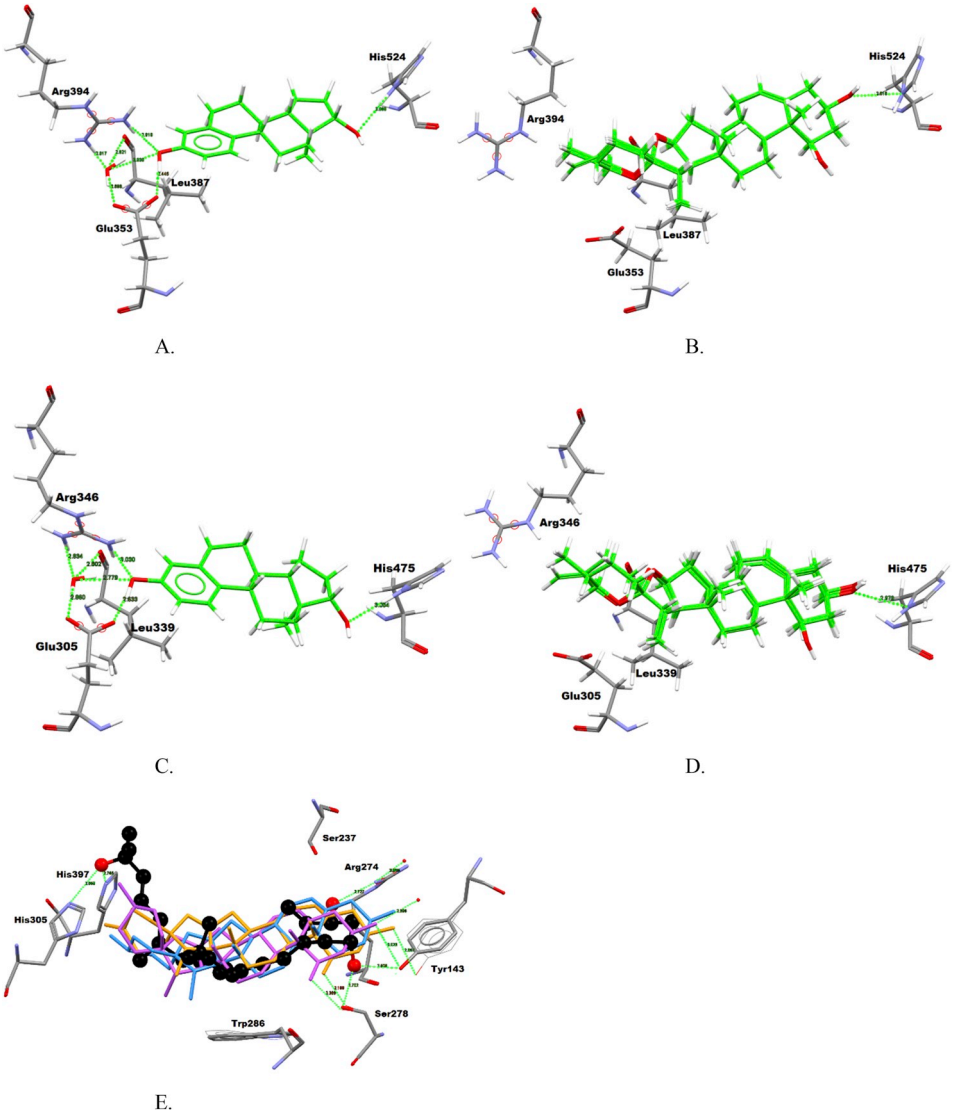

Fig. 10. Docking poses and interactions of EST with ERα (A) and ERβ (C); DSG, RSG, and NRS with ERα (B) and ERβ (D). Docking poses and interactions of VD3 (in black), DSG (in blue), RSG (in pink) and NRS (in orange) with VDR (E). For clarity in (E), the hydrogen atoms are not visualized and the water molecules are given as red points. The hydrogen bonds are shown as green lines. (For interpretation of the references to colour in this figure legend, the reader is referred to the Web version of this article.)

not involved in any hydrogen bond and the closest structural water is absent in this pose. One might conclude that the two hydroxyl groups in RSG and NRG compensate the hydrogen bonds of the 3-OH group in VD3 within the ligand binding site. The lower number of hydrogen bonds between the studied compounds and VDR explain the lower GoldScore values than this of VD3.

4. Discussion

Decreased estradiol level in the menopause leads to decreased bone formation and contribute to osteoporosis later (Meng-Xia and Qi, 2015). Clinical (Vogt et al., 1997) and experimental (Ding et al., 2011; Griffith et al., 2010) studies showed that reduced blood flow is a contributing factor to the decreased bone mineral density (BMD) and occur simultaneously. Griffith and co-workers (Griffith et al., 2010) proved that a reduced amount of erythropoietic marrow and endothelial dysfunction after ovariectomy decrease blood flow. It was shown that hypoxia strongly stimulates the number and size of osteoclasts resulting in increased bone resorption and inhibition of osteoblast activity (Marenzana and Arnett, 2013). Therefore, drugs or plant-derived bioactive substances that increase blood supply to the bones might be useful for prevention of the osteoporosis.

Based on the above-mentioned data the purpose of the present work was to evaluate and to compare the effects of the well-known angioprotective and veinotonic extract from *Ruscus aculeatus* extract (ERA), the sapogenin diosgenin, and antiresorptive bisphosphonate alendronate on the bones of ovariectomized (OVX) female Wistar rats.

Bilateral ovariectomy is a widely used model for evaluation of postmenopausal osteoporotic complications and the effects of synthetic or naturally occurring compounds on the osteoporotic changes. It has been established that the decline of estradiol level is a key mechanism leading to increased body mass, decreased bone mass, and induced oxidative stress (OS). In our study, the estradiol (EST) levels in all animal groups were very low (Table 3). Probably the EST insufficiency in the OVX rats is the main contributing factor for the significant body weight gain (Table 1), enhancement of the formation of lipid peroxides, measured as MDA equivalents (Fig. 3A) and decreased the quantity of the main endogenous antioxidant and cell protector GSH (Fig. 3B). According to (Oršoli'c et al., 2018) reactive oxygen species (ROS) are involved in estrogen deficiency-induced bone loss through increased osteoclast activity leading to an imbalance between the formation and resorption of the bones Sapcota and co-workers showed that natural compounds as thymol may inhibit osteoclast activity and thus inhibit bone resorption process through different mechanisms (Sapkota et al., 2018).

R. aculeatus preparations are widely distributed in Europe and have been used for more than 40 years to treat chronic venous insufficiency and vasculitis (Huang et al., 2008). The main active constituents of the plant and carriers of those effects are the steroid saponins ruscogenin and neoruscogenin. Extract from the underground parts of *R. aculeatus* (ERA) used in this study was standardized to 20% steroidal heterosides, expressed as RSG and NRS, according to Pharmacopoeia method. As evidenced by the *in vitro* study on SAOS-2 cell line ERA demonstrated an osteoblastogenic effect similar to diosgenin. When comparing changes in metabolic activity of SAOS-2 cell line at different concentrations of DSG and ERA, a strong correlation was observed. The stated similarities in cell response patterns were rather predictable because of the structural similarity between the tested compounds. Structures of RSG and NRS (the main sapogenins in ERA) are very close to diosgenin's structure (Fig. 1). Based on our own experimental findings, a similar to diosgenin's beneficial effect on bone turnover could be ascribed to ERA due to its high content of spirostanol saponins. The documented inhibitory effect of the extract at the highest exposure level, on the other hand, is most likely associated with the complex composition of the extract and its multimodal biological properties.

In the present study, the markers of calcium and bone homeostasis were also significantly disturbed in OVX rats at the 35th day from the beginning of the experiment (Tables 2 and 3). Administration of ERA at 100 and 200 mg/kg, as well as DSG, normalized the bone formation, discerned by amelioration of the bone turnover markers (Table 3), radiological (Figs. 4–7) and histological changes (Figs. 8 and 9) in OVX rats and by reducing the OVX-induced oxidative stress (Fig. 3). The beneficial effects of ERA established in this research could be due not only to its osteogenic potential but also to its effects on the circulatory system. The vasoconstriction produced by *R. aculeatus* in the peripheral vessels might redistribute the blood in the body and to increase blood supply to the bones.

Additionally, in the review of Howes (2018), it is stated that RSG could downregulate NF-κB-stimulated inflammatory responses in experimental animal models and suppress the inflammation via inhibition of NF-κB-mediated inflammatory gene expression. Osteoclasts formation requires nuclear factor-kappa B (NF-κB) signalling. Therefore, the inhibition of this signal molecule might decrease the osteoclast proliferation, differentiation and activity and to slow down the bone resorption, which supports our radiological (Figs. 4–7) and histological (Figs. 8 and 9) data for the bone-protective effects of ERA.

Calcium plays a vital role in the development, growth, and maintenance of bone health. Around 99% of the calcium in the body is found in the bones. Calcium in the blood is maintained within a very narrow range and stable concentration. Uribe and colleagues (Uribe et al., 2011) reported that the reference values of Ca^{2+} in adult Wistar rats are 0.85 mmol/L. According to Wang et al. (2002) the normocalcaemic level in Wistar rats is of 1.27 ± 0.02 mmol/L. In the present study, the Ca^{2+} level in OVX groups, treated with both doses of ERA and DSG, on the 35th day was higher than 2.6 mmol/L (Table 2). Obviously, the increased bone turnover following estrogen deprivation after OVX is one of the reasons for this hypercalcemia. From the other side, the increased Ca level might be due to the increased intestinal Ca absorption due to the ameliorated antioxidant status of the GUT by ERA (Fig. 3). According to Diaz de Barboza (Diaz de Barboza et al., 2017) intestinal Ca^{2+} absorption depends on the of GSH content and GSH deficiency can inhibit the intestinal Ca^{2+} absorption by modifying the pathways and molecules involved in its transfer. Some saponins could enhance intestinal absorption (Chao et al., 1998; Johnson et al., 1986) and thus increase the bioavailability of insufficiently or poorly absorbed micronutrients such as calcium. Some data show that saponins might increase the body's ability to absorb calcium (Ewart, 1931; Cheruiyot, 2009). A number of investigators have shown the powerful antioxidant and organ-protective effects of *Ruscus* extracts (de Almeida Cyrino et al., 2018) and diosgenin (Selim and Al Jaouni, 2016). The results from the present study indicated that ERA, administered at higher doses (100 and 200 mg/kg), as well as DSG, significantly increased the GSH content in the liver and intestines (Fig. 3B) which in turn might increase Ca^{2+} intestinal intake as opposed to ALN, which showed pro-oxidant effects, assessed by the rise of MDA quantity and depletion of GSH content (Fig. 3).

The chemical composition of the rhizomes and roots of *R. aculeatus* is well known – the species has been reported to contain steroidal saponins, but the information of the other constituents is limited. This is also valid for the pharmacological action of the plant. Most of the investigations have been based on venotonic and antithrombotic effects (Masullo et al., 2016). Ethanolic extracts of *R. aculeatus* were proved to contain sterols, anthraquinones and volatile oils (Nikolov, 2006). Their antioxidant activity *in vitro* was also reported (Jakovljevic et al., 2015). Due to the anti-inflammatory activity of steroidal saponins, including ruscogenins (Huang et al., 2008) the observed antiosteoporotic effects could be directly assigned to them. Moreover, the defatting procedure for ERA preparation eliminated the possibility of sterols or volatiles to be present in ERA.

The key regulators of calcium homeostasis in the body are parathyroid hormone (PTH) and $1,25(OH)_2D3$ (the active form of vitamin D). The hypercalcemia detected in the study suppresses the secretion of

the parathyroid hormone (PTH) (Table 2), which in turn decrease the formation of the active form 1,25 $(OH)_2$ D_3 in the kidney. A 25(OH) D level of less than 25 nmol/L in serum was considered to be vitamin D deficiency (Lips, 2001). In the present study, only the OVX group and the lower doses (50 and 100 mg/kg) ERA-treated OVX group showed vit. D serum level below 25 nmol/L (Table 2).

The *in silico* target prediction by SwissADME tool (http://www.swissadme.ch/index.php) showed that the main ERA saponins RSG and NRS could bind to Vit. D receptor and affect the Ca absorption or estradiol synthesis (Mutchie et al., 2019). The ability of RSG and NRS to bind in Vit. D receptor was confirmed in our experiments by molecular docking.

Probably because of the faster bone turnover rate in rats (Rissanen, 2013), in the present study the biochemical markers were restored to the normal level at the end of the 10th week. According to Chan and Swaminathan, rapid bone loss is seen immediately after OVX (Chan and Swaminathan, 1998). After this period the calcium homeostasis is maintained within very narrow limits by the participation of PTH and 1,25-OH Vit. D.

Our finding demonstrated that the treatment with the higher doses (100 and 200 mg/kg) ERA, DSG, and ALN significantly inhibited the bone turnover markers such as ALP, OC, and CTx levels in the serum compared to the OVX group at the 35th day (Table 3). These results show that ERA can exhibit, in addition to the antioxidant and osteogenic effect, an estradiol-like effect. The molecular docking of DSG, RSG, and NRS on ERα, ERβ, and VDR showed that these compounds bind in a similar way as EST but with lower scores due to the lower number of hydrogen bonds with the receptors. Nevertheless, the *in silico* correlations found could not be attributed to the overall effects of ERA. *In vivo* biotransformation, both in the digestive tract and on the cellular level could modify the response. Moreover, the steroidal saponins constitute 20% of ERA, thus other ingredients are to be identified in the next studies.

The structural similarity between EST, DSG and ruscogenins explain the dose-dependent bone protective effects of ERA and show that *R. aculeatus* might be a useful source for the development of effective prophylactic treatment of age-associated osteoporosis. According to our study, ERA is an effective antioxidant with potential estrogenic, vit. D-like, and osteoblast activity. It could potentially protect against age-associated bone loss or bone loss induced by OVX and by increasing calcium intestinal absorption.

5. Conclusions

For the first time, the anti-osteoporotic activity of ERA has been reported and the main bioactive substances have been docked to estrogen receptors (alfa and beta) and to Vit. D receptor (VDR). Our findings suggest that ERA and DSG demonstrate a significant antioxidant and antiosteoporotic effect in OVX-induced osteoporotic rats by maintaining calcium and phosphorus homeostasis, by increasing of the antioxidant potential that augments bone markers formation and bone mineral density and by reducing the induced lipid peroxidation and bone resorption. The bone protective action of the ERA could be attributed to:

- Stimulation of osteoblastogenesis and bone formation;
- Intestinal antioxidant effect helping the Ca intestinal absorption;
- *In silico* predicted VDR binding affinity and thus increasing Ca absorption;
- *In silico* predicted ER binding affinity and thus stimulating the bone formation and decreasing the bone resorption;
- NF-κB inhibition and thus anti-inflammatory action, suppressing osteoclast activity
- Increased blood circulation to the bones or blood supplying effects.

Conflicts of interest

The authors declare no conflict of interests.

Declaration of interests

The authors declare that they have no known competing financial interests or personal relationships that could have appeared to influence the work reported in this paper.

Acknowledgments

The study was supported by Grant “Young scientist” Contract № D-128/2019, Project № 8233/20.11. 2018, from the Council of Medical Science, Medical University of Sofia.

References

Bancroft, J.D., Gamble, M. (Eds.), 2008. Theory and Practice of Histological Techniques. Elsevier health sciences.

Bazzigaluppi, P., Adams, C., Koletar, M.M., Dorr, A., Pikula, A., Carlen, P.L., Stefanovic, B., 2018. Oophorectomy reduces estradiol levels and long-term spontaneous neurovascular recovery in a female rat model of focal ischemic stroke. Front. Mol. Neurosci. 11 article 338. http://doi.10.3389/fnmol.2018.00338.

Bump, E.A., Taylor, Y.C., Brown, J.M., 1983. Role of glutathione in the hypoxic cell cytotoxicity of misonidazole. Cancer Res. 43 (3), 997–1002. http://www.ncbi.nlm.nih.gov/pubmed/6825119.

Chakuleska, L., Simeonova, R., Danchev, N., 2018. Review on the pharmacology of osteoporosis. Pharmacia 65 (3), 49–56.

Chan, E.L., Swaminathan, R., 1998. Calcium metabolism and bone calcium content in normal and oophorectomized rats consuming various levels of saline for 12 months. J. Nutr. 128 (3), 633–639. https://doi.org/10.1093/jn/128.3.633.

Chao, A., Vu Nguyen, J.V., Broughall, M., Recchia, J., Kensil, C.R., Daddona, P.E., Fix, J.A., 1998. Enhancement of intestinal model compound transport by DS-1, a modified Quillaja saponin. J. Pharm. Sci. 87 (11), 1395–1399. https://doi.org/10.1021/js9800735.

Cheng, Y.Y., Huang, L., Lee, K.M., Li, K., Kumta, S.M., 2004. Alendronate regulates cell invasion and MMP-2 secretion in human osteosarcoma cell lines. Pediatr. Blood Canc. 42, 410–415. https://doi.org/10.1002/pbc.20019.

Cheruiyot, K.J., 2009. Physical-chemical and Bioactivity Investigations of Anti-diabetic Traditional Drugs. Thesis for MSc University of Nairobi, pp. 32.

Cos, P., De Bruyne, T., Apers, S., Vanden Berghe, D., Pieters, L., Vlietinck, A.J., 2003. Phytoestrogens: recent developments. Planta Med. 69 (7), 589–599. https://doi.org/10.1055/s-2003-41122.

de Almeida Cyrino, F.Z.G., Balthazar, D.S., Sicuro, F.L., Bouskela, E., 2018. Effects of venotonic drugs on the microcirculation: comparison between Ruscus extract and micronized diosmine. Clin. Hemorheol. Microcirc. 68 (4), 371–382. https://doi.org/10.3233/CH-170281.

Denova-Gutiérrez, E., Méndez-Sánchez, L., Muñoz-Aguirre, P., Tucker, K.L., Clark, P., 2018. Dietary patterns, bone mineral density, and risk of fractures: a systematic review and meta-analysis. Nutrients 10 (12), E1922. https://doi.org/10.3390/nu10121922.

Derelanko, M.J., Hollinger, M.A., 2002. Handbook of Toxicology, second ed. .

Diaz de Barboza, G., Guizzardi, S., Moine, L., Tolosa de Talamoni, N., 2017. Oxidative stress, antioxidants, and intestinal calcium absorption. World J. Gastroenterol. 23 (16), 2841–2853. https://doi.org/10.3748/wjg.v23.i16.284.

Diaz de Barboza, G., Guizzardi, S., Nori Tolosa de Talamoni, N., 2015. Molecular aspects of intestinal calcium absorption. World J. Gastroenterol. 21 (23), 7142–7154. https://doi.org/10.3748/wjg.v21.i23.7142.

Ding, W.G., Wei, Z.X., Liu, J.B., 2011. Reduced local blood supply to the tibial metaphysis is associated with ovariectomy-induced osteoporosis in mice. Connect. Tissue Res. 52, 25–29. https://doi.org/10.3109/03008201003783011.

Europe Council, 2017. European Pharmacopoeia 9.0. Council Of Europe: European Directorate for the Quality of Medicines and Healthcare, Strasbourg.

Ewart, A.J., 1931. The Poisonous Action of Ingested Saponins. Commonwealth of Australia: Council for Scientific and Industrial Research Bull No. 50.

Folwarczna, J., Zych, M., Nowińska, B., Pytlik, M., Bialik, M., Jagusiak, A., Lipecka-Karcz, M., Matysiak, M., 2016. Effect of diosgenin, a steroidal sapogenin, on the rat skeletal system. Acta Biochim. Pol. 63 (2), 287–295. https://doi.org/10.18388/abp.2015_1095.

Griffith, J.F., Wang, Y.X.J., Zhou, H., Kwong, W.H., Wong, W.T., Sun, Y.L., Huang, Y., Yeung, D.K., Qin, L., Ahuja, A.,T., 2010. Reduced bone perfusion in osteoporosis: likely causes in an ovariectomy rat model. Radiology 254, 739–746. https://doi.org/10.1148/radiol.09090608.

Halabe, A., Lifschitz, B.M., Azuri, J., 2000. Liver damage due to alendronate. N. Engl. J. Med. 343 (5), 365–366. https://doi.org/10.1056/NEJM200008033430512.

Hernlund, E., Svedbom, A., Ivergard, M., Compston, J., Cooper, C., Stenmark, J., McCloskey, E.V., Jonnson, B., Kanis, J.A., 2013. Osteoporosis in the European Union: Medical management, epidemiology, and economic burden. Arch. Osteoporosis. 8 (1–2), 136. https://dx.doi.org/10.1007/s11657-013-0136-1.

Howes, M.J.R., 2018. Phytochemicals as anti-inflammatory nutraceuticals and phytopharmaceuticals. In: Immunity and Inflammation in Health and Disease. Emerging Roles of Nutraceuticals and Functional Foods in Immune Support, pp. 363–388. https://doi.org/10.1016/b978-0-12-805417-8.00028-7.

Huang, Y.L., Kou, J.P., Ma, L., Song, J.X., Yu, B.Y., 2008. Possible mechanism of the anti-inflammatory activity of ruscogenin: role of intercellular adhesion molecule-1 and nuclear factor-κB. J. Pharmacol. Sci. 108, 198–205. https://doi.org/10.1254/jphs.08083FP.

Ivanova, S., Vasileva, L., 2017. Current and emerging strategies in osteoporosis management. Curr. Pharmaceut. Des. 23 (41), 6279–6287. https://doi.org/10.2174/1381612823666170714122714.

Jakovljevic, V., Milicevic, J., Djelic, G., Vrvic, M., 2015. Antioxidant activity of Ruscus species from Serbia; Potential new sources of natural antioxidants. Hem. Ind. 70, 13. https://doi.org/10.2298/HEMIND140830013JJ.

Johnson, I.T., Gee, J.M., Price, K., Curl, C., Fenwick, G.R., 1986. Influence of saponins on gut permeability and active nutrient transport in vitro. J. Nutr. 116 (11), 2270–2277. https://doi.org/10.1093/jn/116.11.2270.

Kander, M.C., Cui, Y., Liu, Z., 2017. Gender difference in oxidative stress: a new look at the mechanisms for cardiovascular diseases. J. Cell Mol. Med. 21 (5), 1024–1032. https://doi.org/10.1111/jcmm.13038.

Lips, P., 2001. Vitamin D deficiency and secondary hyperparathyroidism in the elderly: consequences for bone loss and fractures and therapeutic implications. Endocr. Rev. 22, 477–501. https://doi.org/10.1210/edrv.22.4.0437.

Lorke, D., 1983. A new approach to practical acute toxicity testing. Arch. Toxicol. 54 (4), 275–287.

Marenzana, M., Arnett, T.R., 2013. The key role of the blood supply to bone. Bone Res. 3, 203–215. https://doi.org/10.4248/BR201303001.

Masullo, M., Pizza, C., Piacente, S., 2016. Ruscus genus: a rich source of bioactive steroidal saponins. Planta Med. 82, 1513–1524. https://doi.org/10.1055/s-0042-119728.

Meng-Xia, J., Qi, Y., 2015. Primary osteoporosis in postmenopausal women Chronic. Dis. Translat. Med. 1 (1), 9–13. https://dx.doi.org/10.1016/j.cdtm.2015.02.006.

Men-Luh, Y., Jen-Liang, S., Chung C., L., Kuang T., W., Ching Y., Y., Wei C., F., Chiao C., C., Min K., L., 2005. Diosgenin induces HIF-1 activation and angiogenesis through estrogen receptor-related PI3K/Akt and p38 MAPK pathways in osteoblasts. Mol. Pharmacol. 68 (4), 1061–1073. https://doi.org/10.1124/mol.104.010082.

Möcklinghoff, S., Rose, R., Carraz, M., Visser, A., Ottmann, C., Brunsveld, L., 2010. Synthesis and crystal structure of a phosphorylated estrogen receptor ligand binding domain. Chembiochem 11 (16), 2251–2254. https://doi.org/10.1002/cbic.201000532.

Mustafa, R.A., Alfky, N.A., Hijazi, H.H., Header, E.A., Azzeh, F.S., 2018. Biological effect of calcium and vitamin D dietary supplements against osteoporosis in ovariectomized rats. Prog. Nutr. 20, 86–93. https://doi.org/10.23751/pn.v20i1.5223.

Mutchie, T.R., Yu, O.B., Di Milo, E.S., Arnold, L.A., 2019. Alternative binding sites at the vitamin D receptor and their ligands. Mol. Cell. Endocrinol. 485, 1–8. https://doi.org/10.1016/j.mce.2019.01.011.

Nikolov, S.D. (Ed.), 2006. Specialized Encyclopaedia of Medicinal Plants in Bulgaria. Labour Publishing House, Sofia.

Oršolić, N., Nemrava, J., Jeleč, Ž., Kukolj, M., Odeh, D., Terzić, S., Fureš, R., Bagatin, T., Bagatin, D., 2018. The beneficial effect of proanthocyanidins and icariin on biochemical markers of bone turnover in rats. Int. J. Mol. Sci. 19 (9), 2746. https://doi.org/10.3390/ijms19092746.

Peneva, B., Krasteva, I., Nikolov, S., Minkov, E., 2000. HPTLC densitometric determination of ruscogenins in dry extract of Ruscus aculeatus L. Pharmacia 55, 541–542.

Polizio, H.A., Peña, C., 2005. Effects of angiotensin II type 1 receptor blockade on the oxidative stress in spontaneously hypertensive rat tissues. Regul. Pept. 128 (1), 1–5. https://doi.org/10.1016/j.regpep.2004.12.004.

Rauly-Lestienne, I., Heusler, P., Cussac, D., Lantoine-Adam, F., de Almeida Cyrino, F.Z., Bouskela, E., 2017. Contribution of muscarinic receptors to in vitro and in vivo effects of Ruscus extract. Microvasc. Res. 114, 1–11. https://doi.org/10.1016/j.mvr.2017.05.005.

Rissanen, J., 2013. Markers of Bone Turnover in Preclinical Development of Drugs for Skeletal Diseases. Ph.D. thesis. vol. 14. University of Turku, Turku, Finland, pp. 47 16.

Rochel, N., Wurtz, J.M., Mitschler, A., Klaholz, B., Moras, D., 2000. The crystal structure of the nuclear receptor for vitamin D bound to its natural ligand. Mol. Cell 5 (1), 173–179. https://doi.org/10.1016/S1097-2765(00)80413-XX.

Sapkota, M., Li, L., Kim, S.W., Soh, Y., 2018. Thymol inhibits RANKL-induced osteoclastogenesis in RAW264.7 and BMM cells and LPS-induced bone loss in mice. Food Chem. Toxicol. 120, 418–429. https://doi.org/10.1016/j.fct.2018.07.0322.

Selim, S., Al Jaouni, S., 2016. Anti-inflammatory, antioxidant and antiangiogenic activities of diosgenin isolated from traditional medicinal plant, *Costus speciosus* (Koen ex. Retz) Sm. Nat. Prod. Res. 30 (16), 1830–1833. https://doi.org/10.1080/14786419.2015.1065493.

Speltz, T.E., Mayne, C.G., Fanning, S.W., Siddiqui, Z., Tajkhorshid, E., Greene, G.L., Moore, T.W., 2018. A "cross-stitched" peptide with improved helicity and proteolytic stability. Org. Biomol. Chem. 16 (20), 3702–3706. https://doi.org/10.1039/c8ob00790j.

SwissADME tool. http://www.swissadme.ch/index.php.

Tao, X., Qi, Y., Xu, L., Yin, L., Han, X., Xu, Y., Wang, C., Sun, H., Peng, J., 2016. Dioscin reduces ovariectomy-induced bone loss by enhancing osteoblastogenesis and inhibiting osteoclastogenesis. Pharmacol. Res. 108, 90–101. https://doi.org/10.1016/j.phrs.2016.05.003.

Tobyn, G., 2013. Culpeper's Medicine: a Practice of Western Holistic Medicine, new edition. Singing Dragon, Jessika Kingsley Publishers, London, UK, pp. 214.

Turner, J.V., Agatonovic-Kustrin, S., Glass, D.B., 2007. Molecular aspects of phytoestrogen selective binding at estrogen receptors. J. Pharm. Sci. 96 (8), 1879–1885. https://doi.org/10.1002/jps.20987.

Uribe, E.R., Aparicio, P.S., Izquierdo, A.C., Rodríguez, A.A., 2011. Reference values for electrolytes and blood gases in Wistar rats with permanent cerebral ischemia: the effect of treatment with glycine on gasometry and electrolytes. Multiciencias 4 (378 – 386).

Vogt, M.T., Cauley, J.A., Kuller, L.H., Nevitt, M.C., 1997. Bone mineral density and blood flow to the lower extremities: the study of osteoporotic fractures. J. Bone Miner. Res. 12, 283–289. https://doi.org/10.1359/jbmr.1997.12.2.283.

Wang, W., Lewin, E., Olgaard, K., 2002. Role of calcitonin in the rapid minute-to-minute regulation of plasma Ca2+ homeostasis in the rat. Eur. J. Clin. Investig. 32, 674–681. https://doi.org/10.1046/j.1365-2362.2002.01054.

Zheng, X., Lee, S.K., Chun, O.K., 2016. Soy isoflavones and osteoporotic bone loss: a review with an emphasis on modulation of bone remodeling. J. Med. Food 19 (1), 1–14. https://doi.org/10.1089/jmf.2015.0045.